Reliability Engineering and System Safety 144 (2015) 254–264

Contents lists available at ScienceDirect

Reliability Engineering and System Safety

journal homepage: www.elsevier.com/locate/ress

Probabilistic modelling of security of supply in gas networks and evaluation of new infrastructure

Pavel Praks, Vytis Kopustinskas*, Marcelo Masera

European Commission, Joint Research Centre, Institute for Energy and Transport, E. Fermi 2749, TP230, I-21027 Ispra, VA, Italy

ARTICLE INFO

Article history:
Received 25 February 2015
Received in revised form
24 June 2015
Accepted 5 August 2015
Available online 15 August 2015

Keywords:
Gas transmission network modelling
Network reliability
Network resilience
Monte-Carlo methods

ABSTRACT

The paper presents a probabilistic model to study security of supply in a gas network. The model is based on Monte-Carlo simulations with graph theory, and is implemented in the software tool ProGasNet. The software allows studying gas networks in various aspects including identification of weakest links and nodes, vulnerability analysis, bottleneck analysis, evaluation of new infrastructure etc. In this paper ProGasNet is applied to a benchmark network based on a real EU gas transmission network of several countries with the purpose of evaluating the security of supply effects of new infrastructure, either under construction, recently completed or under planning. The probabilistic model enables quantitative evaluations by comparing the reliability of gas supply in each consuming node of the network.

1. Introduction

A number of energy supply disruptions due to economic, political or technical reasons highlight the need to study energy infrastructure networks from the security of supply point of view. After supply disruption in January 2009 due to the Russia-Ukraine dispute, the European Commission reacted by issuing Regulation 994/2010 on security of gas supply [1], which requires the EU Member States to fulfil a number of requirements, including risk assessment, preventive action plan and emergency action plan, installation of cross border reverse flow capabilities, and supply and infrastructure standards, including the N-1 criterion. These and other measures proved to be important for the gas network resilience in the subsequent smaller supply disruptions (e.g. Libyan war in 2011, cold snap in early 2012). As energy security remains on the top priority list of the European Commission, several actions are planned including revision of the Regulation [1], funding construction of new infrastructure, adoption of energy security strategy and finally creation of Energy Union.

A gas transmission network can be understood as a critical infrastructure, an issue that has been recently addressed by various initiatives from research institutions and governments worldwide. The European Commission has taken the initiative to organise a network consisting of research and technology organisations within the European Union with interests and capabilities in critical infrastructure protection [2]. Interdependencies between critical infrastructures make the analysis complicated and challenging, but the topic has attracted a growing number of researchers [3–5]. For energy infrastructures the most interesting interdependence is between gas and electricity networks, as discussed in the benchmark study presented in [6].

Reliability, risk and security of supply analyses of energy infrastructure networks present a number of challenges as many network analysis algorithms (optimal distribution of capacity, rerouting of flows etc.) originally developed for telecommunication networks are not directly applicable to gas transmission networks. Detailed analysis of large networked systems is being addressed by a growing number of researchers. From the computational point of view, large network analysis is very demanding; however increased power of modern computers makes complex studies feasible.

A detailed review of the state of the art in the field of network reliability analysis is reported in [7] in which computational complexity, exact algorithms, analytic bounds and Monte Carlo (MC) methods are presented. Availability evaluation of gas transportation is analysed in [8]. Reliability and vulnerability analysis of networks with application to power system is shown in [9]. Reliability of multi-state flow networks has been recently analysed in [10].

The paper [11] focuses on developing a simulation model for the analysis of transmission pipeline network with detailed characteristics of compressor stations. The simulation model is used to create a system that simulates the network with different configurations to get pressure and flow parameters.

The authors analyse gas networks with inclined pipes [12]. The resulting set of fluid flow governing equations is highly non-linear. The authors introduce a novel linear-pressure analogue method,

* Corresponding author.
E-mail addresses: pavel.praks@jrc.ec.europa.eu (P. Praks), vytis.kopustinskas@jrc.ec.europa.eu (V. Kopustinskas), marcelo.masera@ec.europa.eu (M. Masera).

http://dx.doi.org/10.1016/j.ress.2015.08.005

which is compared with the Newton–Raphson nodal method. The proposed solution methodology retains most advantages of the Newton-nodal method while removing the need for initial guesses and eliminating the need for expensive Jacobian formulations and associated derivative calculations.

Cost-related objectives for gas transmission pipelines network design and planning are analysed in [13]. In this task, the type, location, and installation schedule of major physical components of a network including pipelines and compressor stations are assumed. The authors propose an integrated non-linear optimisation model for this problem.

Taking as examples the power and gas transmission systems in Harris County, Texas, USA, optimum interface designs under random and hurricane hazards are discussed in [14]. To model the gas pipeline operation, the maximum flow algorithm is used. The paper goes beyond previous studies focused only on connectivity.

The book [15] addresses a gap in current network research by developing the theory, algorithms and applications related to repairable flow networks and networks with disturbed flows. According to the author, the potential application of repairable flow networks reaches across many large and complex systems, including active power networks, telecommunication networks, oil and gas production networks, transportation networks, water supply networks, emergency evacuation networks, and supply networks.

This paper presents a probabilistic model to study security of supply in a gas network. The model is based on Monte-Carlo simulations with graph theory, and is implemented in the software tool ProGasNet. This paper also presents a development process and application study of the ProGasNet software tool to the European gas transmission network for the analysis of security of supply. The ProGasNet software is currently under development. The purpose is to develop a mathematical model of a flow network that could be used for many different purposes including reliability of supply at each consuming node, vulnerability analysis, bottleneck analysis, time-dependent gas storage analysis [29] or evaluation of new infrastructure, either real or virtual. The JRC report [16] presents the validation results of two approaches implemented for relatively simple benchmark network systems: Monte-Carlo (MC) reliability simulation and fault tree (FT) analysis, see also [30]. The results of test cases indicate the potential of both methods for network reliability analysis and the need for further research [17].

The purpose of the paper is to

- Develop a Monte-Carlo simulation algorithm for stochastic network model with a priority supply pattern (Section 2).
- To introduce a probabilistic approach for modelling of key gas transmission network components (Section 3).
- To define a real-world EU gas transmission network (Section 4) under selected disruption case studies (Section 5).
- And finally, to present results of numerical experiments in terms of security of supply at each consuming node, which can be used also for vulnerability ranking of disruption case studies (Section 6.1. Quantification of gas supply), redundancy analysis of gas sources (Section 6.2. Quantification of redundancy of gas sources), and evaluation of new infrastructure, either real or virtual (Section 6.3. Quantification of probabilistic effects of a new gas infrastructure).

The presented Monte-Carlo simulation technique for stochastic network model with a priority supply pattern represents a general approach, which can be used for security of supply modelling of various transportation networks (crude oil, water).

2. Monte-Carlo simulation technique for stochastic network model

2.1. Maximum flow algorithm

An important characteristic of a network is its capacity to carry flow. What, given capacities on the arcs, is the maximum flow that can be sent between any two nodes? The resolution of this so called Maximum Flow (MF) problem describes the optimal use of line capacities and establishes a reference point against which to compare other ways of using the network [18].

The mathematical description of the MF problem is a standard problem in graph theory [19]. The aim of the Maximum flow algorithm is to maximise the value of flow passing from the source node s to the sink node t given the two following constrains:

- Conservation of flows: the sum of the flows entering a node must equal the sum of the flows exiting a node, except for the source node and the sink node.
- Capacity: the flow of an edge is non-negative and cannot exceed its capacity.

The Maximum flow problem can be solved by various approaches, for example by linear programming or with the Ford–Fulkerson algorithm, which finds directed paths from the source node to the sink node with available capacity on edges in this path. In the algorithm, this path-searching process is repeated until no additional flow can be added to this directed path.

The case of multiple sources and sinks, involving several source nodes $s_1, s_2,\ldots, s_k$ and several sink nodes $t_1, t_2,\ldots, t_r$ and where the flow from any source can be sent to any sink, is known as Multiple Sources and Sinks problem, and can be straightforwardly converted into a one-source and one-sink problem [20]: Let us introduce a supersource s (virtual source node) with edges (of unlimited capacity) directed from this supersourse s to all source nodes $s_1, s_2,\ldots, s_k$. Furthermore, let us introduce a supersink t (virtual sink node) with edges (also of unlimited capacity) directed from all sink nodes $t_1, t_2,\ldots, t_r$ to the supersink t. Then the problem of maximising the total value of the flow from all sources is then the same as that of maximising the value of the flow from s to t.

2.2. Modelling of stochastic networks

In this subsection we present a Monte-Carlo simulation based algorithm for stochastic flow networks with priority supply patterns based on the distance from the source node: In order to concurrently model both reliability and capacity constraints of the gas transmission network, we use a stochastic network representation, where each node and edge of the flow network can randomly fail, according to a given probabilistic model of the network component. These component failures in the network are modelled using the Monte-Carlo simulation technique.

The algorithm has these inputs:

- The capacity matrix C that provides information about capacity constraints of the network elements including input source nodes, demand nodes and information about connected pipeline capacities (for example per day).
- The length matrix L that provides information about length of the edges between nodes (expressed for example in km). As the used geographical length is a symmetric relation, in order to save the computer memory, only an upper (or lower) triangular part of matrix L is necessary to store.

The output of the algorithm is an optimal flow matrix F satisfying for each Monte-Carlo step the Maximum flow algorithm

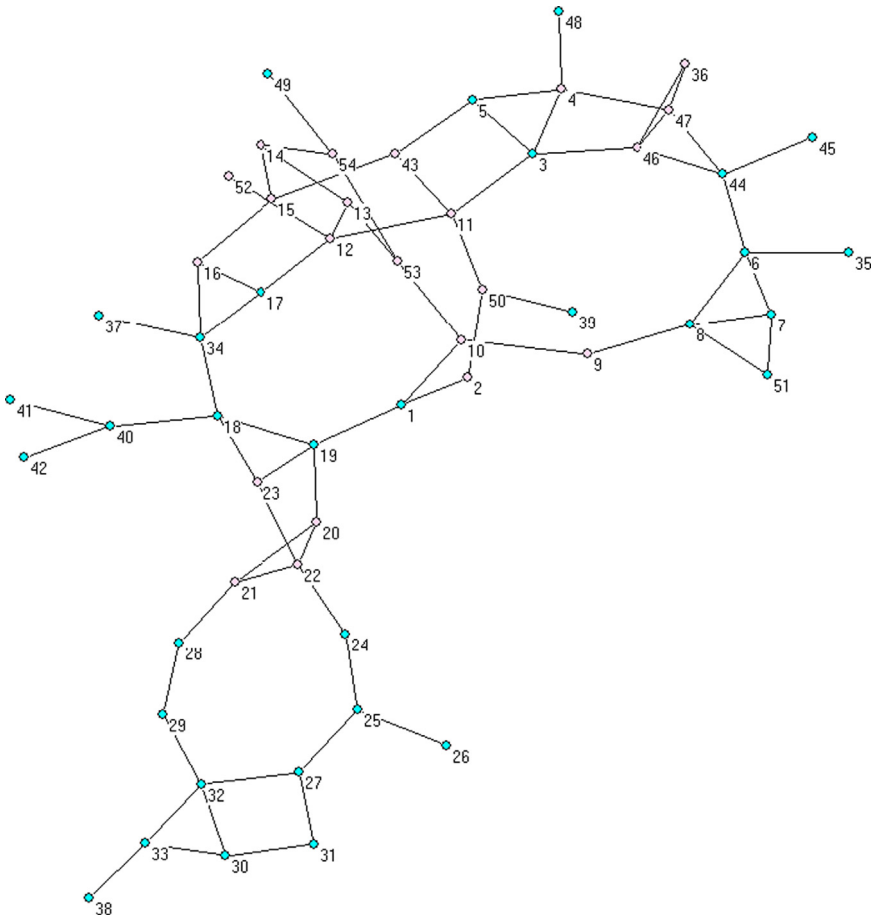

Fig. 1. Anonymized topology of the test gas transmission network.

and the distance based commodity supply pattern, in which the nodes closer to the source are served first.

The implemented priority supply assumption based on geographical distance from the gas source follows the supply gas pattern during previous gas crises in Europe, especially the 2009 Russia-Ukraine gas dispute: The countries geographically far from the blocked gas source were supplied only partially or even were not supplied at all. Of course, this assumption can be easily changed by the user, in order to simulate effects of various supply strategies during the hypothetical gas crises.

In order to correctly model the priority supply pattern based on the distance from the source node for the case of tasks with multiple sources and sinks, one has to introduce additional conditions. For a task with multiple sources, the links between the virtual source node s and the source nodes s_1, s_2,…, s_k are assumed to be unidirectional. It also means that the virtual source node cannot be reached from source nodes. This condition is expressed in the length matrix by the additional penalty:

$$L(s_i, s) = inf, \text{for } i = 1, 2, \ldots, k \quad (1)$$

For a task with multiple sinks, the links between the virtual sink node t and the sink nodes t_1, t_2,…, t_r are assumed to be unidirectional. It means that the sink nodes cannot be reached from the virtual sink node. This penalty is expressed in the length matrix as:

$$L(t, t_i) = inf, \text{for } i = 1, 2, \ldots, r \quad (2)$$

In a case of having multiple sources and multiple sinks, penalties (1) and (2) must be fulfilled simultaneously. In the proposed simulation algorithm, a stochastic flow network is approximated by a sequence of deterministic network flow models. Without losing the generality, the virtual source node is coded in the algorithm by Node 1 (see, for example, node 1 in Fig. 1), whereas the virtual sink node is coded by the symbol t.

In each Monte-Carlo simulation step, the deterministic maximum flow model with sampled component network failures is solved according to the priority supply pattern based on the distance from source. The algorithm uses linear algebra operations for the priority supply pattern, in order to reorder network elements according to the distance based approach. In order to improve the readability of the pseudo-code, the algorithm is expressed in a matrix form, as suggested in [21].

The stochastic flow network algorithm with priority supply pattern based on distance from source includes the following steps:

Input:
Capacity matrix: C
Length matrix: L
Pipeline failure probability per km and year: p_f
Number of Monte-Carlo steps: n_{steps}
Output: optimal flow matrix F satisfying in each Monte-Carlo step the maximum flow according to the distance based commodity supply pattern (nodes closer to the source are served first)

a. $P = initP(L, p_f)$ {*Initialising and defining failure probability matrix of network elements*}.
b. *for* $i = 1,2, \ldots n_{steps}$ {*Main Monte-Carlo loop*}.
c. $C_{rnd} = randpert\ (C, P)$ {*Failed elements have reduced capacity*}.
d. $L_{rnd} = clear\_failured\_elements\ (L, C_{rnd})$ {*Totally failed elements are not reachable*}.

e. $\delta = distance\ (L_{rnd})$.
f. $[_{sorted}, ix] = sort(\delta)$ {*The row vector* δ *is sorted by the ascending order*}.
g. $\Pi = speye(t)$ {*Sparse identity matrix of order t* }.
h. $\Pi = \Pi\ (ix,:\ )$ {*Permutation matrix of elements according to the distance-based approach*}.
i. $C_{rnd} = \Pi \times C_{rnd} \times \Pi^T$ {*Distance -based permutation of the capacity matrix* C_{rnd}}.
j. $f = maxflow\ (1, t, C_{rnd})$.
k. $f = \Pi^T \times f \times \Pi$; {*Inverse transformation of the flow matrix f*}.
l. $F_i = f$
m. *End*

Let us describe the algorithm. Step a is used to define the failure probability matrix P of the network elements. Then in Step b, the Monte-Carlo simulation starts. Network elements, which are stored in the capacity matrix C are subjected to random failures, according to the failure probability matrix P. In Step c the Monte-Carlo sampled capacity matrix is stored in matrix C_{rnd}.

The total failure of the network element causes the component inaccessibility, which can be coded in the algorithm by removing the failed element from the network. For this reason, in Step d the length matrix must be updated. In this way, in case some network component suffers a total failure, the affected network element is not accessible from the source node and the corresponding element of the length matrix L_{rnd} has to be updated.

The algorithm can also be used for modelling the partial failure of a multi-state component, which can be expressed by a partial reduction of the component capacity. Contrary to the total failure, in case of a partial failure the affected network component remains accessible, so the update of the length matrix L_{rnd} in Step d is not necessary.

In Step e the distance vector δ is computed. The vector contains the distance of the shortest paths between the virtual source node and all remaining non-virtual nodes. An entry j of vector δ represents the distance of the shortest path from the virtual source Node 1 to Node j. We used the Matlab tool Bctnet of [26], based on Dijkstra's algorithm. Contrary to the classical Dijkstra's algorithm, it is not necessary to compute the full distance matrix, as only the distance from the virtual source node is used in our algorithm.

In Step e, the distance vector δ is sorted by the ascending order to vector δ_{sorted}, in order to identify the priority for the node commodity supply, because the network elements geographically close to the source node (minimum distance according to length matrix L) have to be served first. The vector ix contains the indices satisfying $\delta_{sorted} = (ix)$. The criticality of nodes for priority supply pattern is coded by the vector ix. Of course, if there is a need, the vector ix can be updated by the user in Step f of the algorithm, in order to simulate effects of various supply strategies during the hypothetical gas crises.

In Step g the identity matrix Π of order t is created, in order to form the permutation matrix. The matrix Π has initially ones on the main diagonal and zeros elsewhere. In order to save computer memory, one can exploit the sparsity pattern of the matrix Π.

In Step h a permutation matrix Π of a graph isomorphism problem is computed according to the distance from the gas source, in order to transfer the original model to the distance-based approach by a dynamic reordering of the network elements. Columns of the matrix Π are permuted according to the indexes produced in Step f. In Step i, the graph isomorphism task is computed by linear algebra operations [21].

Then, in Step j the flow matrix f of the Maximum flow algorithm is computed. The aim is to maximise the commodity flow from the virtual source Node 1 to the virtual sink Node t, according to given constrains. In our computer implementation, we used the above mentioned Ford–Fulkerson algorithm.

To finish the simulation, in Step k the computed flow matrix is transformed back to the original problem by the inversion linear algebra operation. As the permutation matrix Π is sparse and orthogonal, the linear algebra operations are very fast and stable.

Finally, the output optimal flow matrix F is updated in Step m. The resulting flow matrix F is ready for further exploration by statistical methods enabling the monitoring of the flow patterns generated by the Monte-Carlo simulations.

3. Modelling of gas transmission network components

The capacity constraints of key gas transmission network components, i.e. pipelines (Section 3.1), compressor stations (Section 3.2), gas storages (Section 3.3) and liquefied natural gas (LNG) terminals (Section 3.4), are coded by the capacity matrix C. Capacity of an network component connecting the i-th and j-th network element is coded by $C(i,j)$. The capacity network C does not need to be necessary symmetric: For example, it is not always possible to assume a reverse flow between the i-th and j-th network element, because of technical or contractual constrains.

A failure of a network element is coded by a reduction of the capacity matrix. For example, a component failure leading to impossibility of transport gas from the i-th to j-the network element is coded by a reduction of the capacity to zero: $C(i,j) = 0$.

The failure probability of network elements is coded by the failure probability matrix P. Failure probability of a network component connecting the i-th and j-the network element is coded by $P(i,j)$. The matrix P expresses the annual failure probability of network components. The assumed duration of one simulation is a parameter, which is set by the user. In our paper, the network component failures were simulated on a monthly basis, as we are interested in gas supply situation during the first month of a hypothetical gas crisis.

The knowledge of possible gas supply situations during the first month of a gas crisis is crucial for security of supply in the gas network; see especially Regulation 994/2010 on security of gas supply [1], Article 8.

Currently we do not simulate repair of failed components. A long-time scale integration would need more assumptions that the failed components cannot be recovered during the time scale.

Capacity and flow data is expressed at a daily scale, in order to assume peak gas demand during one “peak” day with extreme high gas demand [1]. We assume that the peak demand is constant during the simulation.

3.1. Probabilistic model of a pipeline

In accordance to the GTE report [25], relationship between the pipeline capacity Q and the pipeline diameter D can be approximated by the following relation:

$$Q \sim D^{\gamma}$$

where: D is the diameter of the pipeline, in metres; Q is estimated capacity of the pipeline, in Nm^3/h; and γ is a constant conversion coefficient of 2.59.

This model prediction can be tuned if prior information is available. For example, the maximum pipeline capacity at the cross border connection point together with the pipeline diameter can be taken from a transmission system operator (TSO) reports. Consequently, the maximum pipeline capacity for a different pipeline diameter within the network can be recomputed by

applying the following formula:

$$\frac{Q_1}{Q_2} = \left(\frac{D_1}{D_2}\right)^{\gamma}$$

where: D_1, D_2 are diameters of the pipelines in comparison, in metres; Q_1, Q_2 are capacities of the pipelines in comparison, in Nm^3/h;

The pipeline failure is modelled by the reduction of the pipeline capacity to zero. According to the EGIG report [22], the average failure frequency of a European gas transmission pipeline is 3.5×10^{-4} per kilometer-year. Let us assume that 10% of the reported failures cause complete rupture of a pipeline. The assumed 10% represents the pipeline rupture, according to the EGIG report. As a result, we set pipeline failure probability as $p_f = 3.5 \times 10^{-5}$ per kilometer-year. Currently one damage level (complete damage) is considered for pipelines. In future, a multi-state approach will be analysed.

3.2. Probabilistic model of a compressor station

It is assumed that a compressor station failure causes the reduction of the capacity of the surrounding pipelines. More precisely, a compressor station failure reduces the inlet pipeline and also the outlet pipeline capacity by 20%. This estimate is based on empirical estimations from known operational cases [28], but physical model simulations could serve as a confirmation for each specific situation.

It is assumed that the annual failure probability of a compressor station is 0.25. This is a conservative estimation obtained by a reliability database from network operators. The compressor station are Nodes 11 and 12 in our model (see Fig. 1). Of course, the proposed algorithm is ready for an interaction with physical models, in order to confirm the specific situations. The modelling of interactions is under development.

3.3. Probabilistic model of gas storage

In case of a gas storage failure, it is assumed that the capacity of the pipeline connected to the gas storage is reduced to zero [29]. According to expert knowledge [4], we set the annual failure probability of the gas storage to 0.10. Gas storage is Node 19 in our model (Fig. 1).

3.4. Probabilistic model of LNG terminal

The LNG terminal is modelled as a special of the gas storage: the LNG terminal is modelled as a gas source that can randomly fail. In case of a LNG component failure, it is assumed that the capacity of the pipeline connected to the LNG terminal is reduced to zero. According to literature indications (e.g. [24]), we set the annual failure probability of the LNG terminal to 0.15. Node 10 is a LNG terminal.

4. Definition of the case-study network

Fig. 1 shows the network topology of the test gas transmission network model used in our study. The test case is based on the real gas transmission network of three countries. The presented supply/demand data sets are realistic; however, its geographical topology is not disclosed for sensitivity reasons. The network contains the following elements: pipelines, compressor stations and the LNG terminal (Node 10).

Node 1 is a virtual gas source. In total, there are 4 supply nodes: 2, 10, 11 and 19 (see Table 1). All numbers are expressed in million of cubic metre per day (mcm/d). Gas source at Node 10 represents an LNG terminal with capacity of 4 mcm/d during the initial phase of construction. However, the maximum designed capacity of LNG is 10.5 mcm/d.

In each test case, different supply nodes are used. For example, in Case A, there are three gas sources: Node 2 (with limit 31 mcm/d), Node 10 (LNG with limit 4 mcm/d) and Node 19 (with limit 25 mcm/d), see Fig. 1. Case F is based on Case A, but the LNG terminal at Node 10 has extended its capacity limit up to 10.5 mcm/d.

Pipeline diameters and their lengths were obtained from the gas operators. Consequently, the respective capacities have been estimated from pipelines diameters according to the GTE report [25], as discussed in Section 2. Moreover, the estimation of the transmission pipeline capacities has been independently verified by the authors and is consistent with results published at reference [23]. All the properties of the transmission gas pipelines are summarised in Table 2. As the matrices C and L are symmetric

Table 1
Properties of the gas sources of the gas network. The physical limits (column limit) of gas sources are expressed in mcm/d.

from	To	limit
1	2	31
1	10	4 or 10.5
1	11	7.1
1	19	25

Table 2
Properties of connected elements of the gas network. Capacities are expressed in mcm/d; lengths are expressed in km.

from	to	capacity	length	from	to	capacity	length
2	50	31	23	18	23	49.16	43
3	4	49.16	0.01	18	34	2.83	43
3	5	12.11	32	18	40	5.05	148
3	11	12.11	29	19	20	12.11	60
3	46	17.13	22	19	23	12.11	0.01
4	5	12.11	32	20	21	49.16	90
4	47	2	22	20	22	12.11	0.01
4	48	12.11	2	21	22	12.11	90
5	43	5.05	5	21	28	12.11	86
6	7	12.11	80	22	23	7	60
6	8	5.05	80	22	24	12.11	86
6	35	5.05	30	24	25	0.83	86
6	44	5.05	11.6	25	26	12.11	46
7	8	49.16	0.01	25	27	49.16	100
7	51	12.11	200	27	31	5.05	0.01
8	9	2.83	25	27	32	5.05	70
8	51	12.11	200	28	29	49.16	50
9	10	2.83	162	29	32	49.16	195
10	53	1.34	144	30	31	5.05	70
10	54	5.05	144	30	32	0.47	0.01
11	12	2	103	30	33	0.47	60
11	43	12.11	34	32	33	2	60
11	50	49.16	31	33	38	5.05	60
12	13	49.16	85	34	37	2.83	200
12	17	49.16	62	36	46	5.05	24
12	52	12.11	10	36	47	5.05	24
13	14	30.6	0.01	39	50	1.34	106
13	53	2	30	40	41	5.05	32
14	15	5.05	85	40	42	12.11	63
14	54	5.05	30	44	45	5.05	1
15	16	12.11	62	44	46	17.13	23
15	43	12.11	132	44	47	2	23
16	17	25	0.01	46	47	49.16	0.01
16	34	4	24	49	54	0.83	40
17	34	12.11	24	53	54	49.16	0.01
18	19	12.11	43				

in our benchmark, only non-zero elements of the upper triangular matrices are shown in Table 2.

Finally, Table 3 illustrates the properties of the demand nodes of the gas network. Node 55 is a virtual sink node. Node demands have been estimated according to partial information obtained from the gas operators. The 'last mile' is not modelled, as only transmission pipelines are represented in the model.

As our benchmark aims at studying the reliability of the gas network, the demands at the nodes are deterministic. For this reason, the length of the connected pipelines of demand nodes is set close to zero, in order to avoid failures of demand nodes. In the software tool, it is set that no pipeline failures are modelled for 0.01 km or shorter pipelines. In order to simplify Fig. 1, the virtual sink node with the relative connections is not shown.

Length data are used for the calculation of the distance from source nodes, in order to model the priority of supply. The demand nodes close to the source are served first. Moreover, length data sets are used for computing pipeline failure probability, as discussed in Section 2.

Moreover, the physical limits of gas sources, capacities of connected elements and node demands are used as constrains for the Maximum flow algorithm.

5. Disruption case studies

In order to simulate the test network reaction to various gas supply disruptions, the seven following scenarios are studied. All the selected scenarios are significant for understanding security of supply effects: The Case A represents the gas system working in normal conditions (business as usual). The Case B represents previous version of the system, in which LNG terminal was missing. The selected scenarios have been chosen in order to analyse consequences of loss of one or more key gas sources (Case C, D, E). Finally, Cases F and G represent a possible future development of the gas system.

- Case A: LNG at Node 10 has an upper limit capacity of 4 mcm/d. No external disruption; i.e. input nodes 2 and 19 are supplied as contracted. The pipeline between Node 10 (LNG) and Node 53 is not considered in the model.
- Case B: As Case A, but there is no LNG at Node 10.
- Case C: External disruption. Only LNG at Node 10 with upper limit of 4 mcm/d is modelled as a gas source. The pipeline between Node 10 (LNG) and Node 53 is not considered in the model.
- Case D: External disruption. Only LNG at Node 10 with upper limit of 10.5 mcm/d is modelled as a gas source.
- Case E: External partial disruption. Only LNG at Node 10 with upper limit of 10.5 mcm/d and gas storage at Node 19 with upper limit 25 mcm/d are modelled as gas sources.
- Case F: LNG at Node 10 has upper limit 10.5 mcm/d. No external disruption, i.e. input nodes 2 and 19 are supplied as contracted.
- Case G: LNG at Node 10 has upper limit 10.5 mcm/d. No external disruption, i.e. input nodes 2 and 19 are supplied as contracted. Moreover, new gas source with the upper limit 7.1 mcm/d is added on Node 11.

In these scenarios, we assume that the network components (pipelines, compressor stations and LNG terminal) might fail according to the probabilistic estimates discussed above. The failure probabilities can be set by the user independently on scenarios. However, in our scenarios, the component failure probabilities are fixed, in order to directly compare consequences of various disruption scenarios.

For each scenario, 1 million Monte-Carlo simulations were run. The analysis calculated the steady state of supply/demand estimated by the Maximum flow algorithm. According to discussion in Section 3, the network component failures were simulated on a monthly basis, while all the capacity and flow data is expressed at a daily scale.

6. Results of Monte-Carlo simulations

In order to study security of supply in a gas network, various gas supply strategies were simulated with the Monte-Carlo approach. Results of Monte-Carlo simulations are presented by means of statistical indicators, for example by the cumulative distribution function (CDF) plots.

The indicators are computed for all required network nodes. By applying more detailed analysis, it is possible to quantify the probabilistic effects of each component of the gas infrastructure, for example, the local (node) effects of a LNG terminal. The detailed results might be important for gas operators, as network nodes may represent key industrial plants, for example gas driven power stations. Readability of detailed results is increased by the risk ratio.

Even more, it is possible to quantify the redundancy of gas sources. This aspect is interesting especially if one adds more gas source nodes, in order to increase the gas delivery probability of the network. We will see that even if the gas network reliability remains approximately the same, the gas delivery in the gas

Table 3
Properties of demand nodes of the gas network. Node demands are expressed by mcm/d; lengths are expressed in km. Note: Demand on the Node 51 is set to zero for cases C, D, E.

from	to	demand	from	to	demand
5	55	3.43	33	55	0.4
6	55	0.57	34	55	1
7	55	0.66	36	55	1.74
10	55	2.02	37	55	1.3
13	55	1.03	39	55	1
17	55	0.46	41	55	0.4
18	55	8.4	42	55	0.5
21	55	0.54	43	55	1.06
25	55	0.6	44	55	2.82
26	55	0.8	47	55	0.68
27	55	3.5	48	55	1.17
28	55	6	51	55	7
30	55	0.4	52	55	0.98

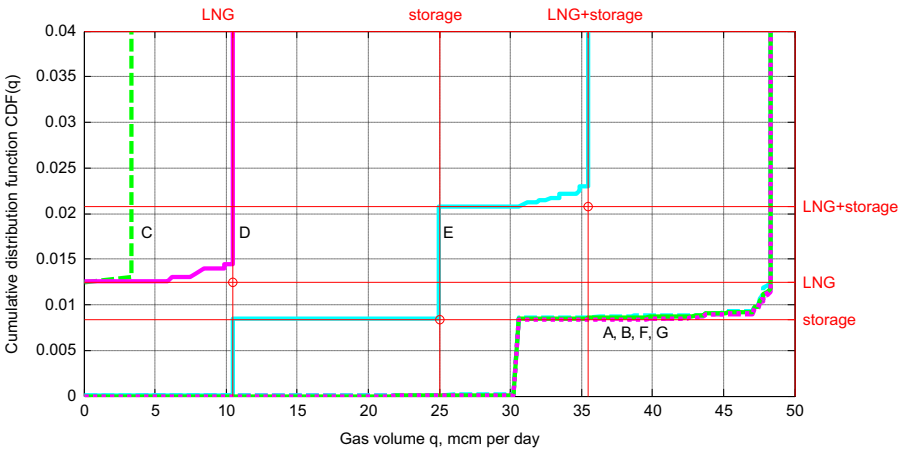

Fig. 2. Global overview: Reliability of gas supply for test cases expressed by truncated CDF.

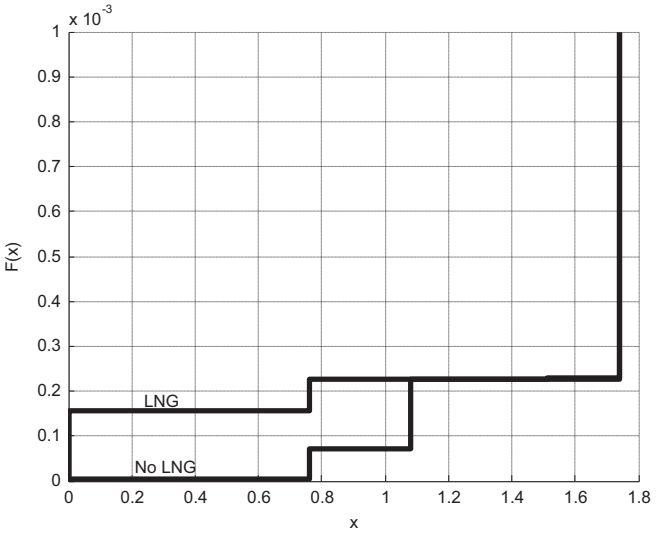

Fig. 3. Reliability of gas supply at Node 36 for Scenario F (with LNG) and Scenario B (No LNG) expressed by the truncated CDF. Although the supply reliability is very large, as we analyse a scenario without external disruption (see small probabilities of order 10^{-3} in the y-axis), it is possible to quantify a positive effect of a 10.5 mcm/d LNG terminal at Node 36.

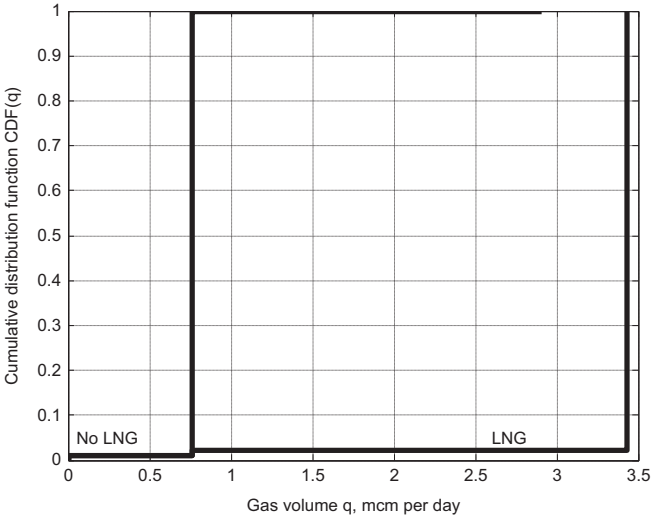

Fig. 4. Reliability of gas supply at Node 5 for Scenario E with LNG and without LNG expressed by the CDF. Although the maximum observed gas supply on the node was 2.91 mcm/d in the case without LNG, gas supply at the node will be only 0.76 mcm/d or less with probability 99.72%. In contrary, with a 10.5 mcm/d LNG terminal, the gas supply will be less than 3.05 mcm/d with only 2.2% probability.

network can be successfully quantified by the probabilistic approach. This probabilistic quantification can be used as a tool for comparing, scoring and ranking different gas infrastructure projects.

6.1. Quantification of gas supply

Fig. 2 shows the cumulative distribution function of the total network supply for all disruption case studies. It can be interpreted as follows: the monthly probability of having less than specific daily demand (gas volume x, on the horizontal axis) is given by the $F(x)$ value (on the vertical axis). We assume that the daily demand is constant during the month.

As expected, the gas supply situation is worse in cases with external gas disruption, i.e. for Cases C and D followed by Scenario E.

In Scenario E, only LNG at Node 10 with upper limit of 10.5 mcm/d and gas storage at Node 19 with upper limit 25 mcm/d are considered as gas sources. The CDF of Scenario E has two very visible 'steps' corresponding to gas volume 10.5 mcm/d and 25 mcm/d. These CDF 'steps' are mainly caused by gas sources failures; this can be verified analytically in an approximate manner, as shown below. (Of course, this consideration is only an approximation, as the failures of the other gas network components, for example the transmission pipeline failures, are assumed only in Monte Carlo simulations, but not in the following roughly analytical verification.)

Let's analyse the CDF 'step' corresponding to gas volume 10.5 mcm/d. This step represents the upper limit of the LNG. This input parameter of the model is shown in the x-axis of the figure by the symbol "LNG". Moreover, the expected monthly failure probability of the LNG is -according to the input data of the model- $0.15/12 = 0.0125$, which is shown by the same symbol "LNG" at the y-axis of the figure. The intersection of these two values is expressed in the figure by a small red circle. In the graph one can see that the CDF for Case D, fully dependent on LNG, is above this circle. This is because CDF includes in all cases internal (random) failures of the gas network elements.

The influence of gas storage is shown by the symbol "storage" in the x-axis with the limit of 25 mcm/d, and in the y-axis by the expected monthly failure probability of the gas storage: $0.10/12 = 0.00833$.

It is evident that the failure of gas storage at Node 19 will cause the loss of 25 mcm/d, and therefore the maximum available supply

will be 10.5 mcm/d, corresponding to the upper limit of the LNG storage. The gas supply will be 10.5 mcm/d or less with probability of 0.0083, as shown in Fig. 2. This probability is consistent with the expected monthly failure probability of the gas storage.

Let us describe the CDF 'step' corresponding to gas volume 25+10.5=35.5 mcm/d. The gas supply will be less than 35.5 mcm/d, when there is a failure of the LNG source (Node 10) or a failure of the gas storage (Node 19):

$$P(Node\ 10 \cup Node\ 19) = P(Node\ 10) + P(Node\ 19) - P(Node\ 10 \cap Node\ 19) = 0.0125 + 0.00833 - 0.0125 * 0.00833 = 0.0207$$

This probability is marked in the *y*-axis of Fig. 2 by the symbol ("LNG+storage"). The same symbol in the *x*-axis of the figure represents the upper limit for LNG and storage: 10.5+25=35.5 (mcm/d). It is visible from the graph that the CDF of the Case E, fully dependent on LNG and storage, is again above the small red circle, as the CDF includes internal (random) failures of the gas network elements.

The cumulative distribution functions of gas supply of the remaining cases (A, B, F, G) are approximately the same, see Fig. 2, as they are not affected by external gas disruptions. In these cases, it is visible that the gas is supplied from the reliable main pipeline source (31 mcm/d of Node 2). Then, in the *x*-axis, at the point corresponding to a gas volume of 31 mcm/d, there is a jump to the storage probability, as for larger volume of gas the system requires supply from the gas storage.

It seems from Fig. 2 that the CDFs of these remaining cases (A, B, F, G) are the same. However, we will see in the next section that these cases are different and this difference can be successfully quantified. For example, the positive impact of LNG is visible also for these cases with no external gas disruptions, when analysing the probabilistic gas supply results at the node level, see Fig. 3. This is due to the fact that LNG can be viewed as a gas local source in our benchmark. Of course, the positive effect of LNG is very visible for a case with the external gas disruption, see Fig. 4.

The Statistical properties of gas supply for the cases presented in this paper are summarised in Table 4. The column "D-mean%" of Table 4 shows the relative difference between demand D and mean value of the supply. The column is expressed as a percentage. The column "cv%" represents the variation coefficient, which is defined as the ratio of the standard deviation "std" to the mean; it is also expressed as a percentage. Results are sorted in the columns "D-mean%" and "cv%". The best case for gas supply appears to be Case G. This is predictable, as this case has the largest redundancy of gas sources (LNG at Node 10 and an additional gas source at Node 11). The set of successful cases ends with Case B. This case has the most limited "redundancy" of gas sources, as there is neither LNG nor any other additional gas source. In Case E, approximately 15% of gas is not supplied in average, because of external gas disruptions. The worst case is again Case C, in which, in average, 90.5% of the demand is not supplied.

Table 5 includes probabilistic results of disruption cases. The table includes for all cases the list of demand quantities (column D) and probabilities that the supply at node *X* will be zero, expressed by the symbol $P(X=0)$, or less than 20%, 50%, 80% or 100% of the node demand.

The results of the disruption cases, with no external gas disruption, fluctuate around the same probabilities – see results of cases A, B, F, G. However, Case B is correctly identified as having the minor value among the cases considered, as it has neither LNG nor any additional gas source.

Case E is able to supply at least 80% of the demand with probability 1-0.0217~0.978. This probability is, approximately, a complement of the 0.0207 probability of the already discussed "LNG+storage" effect, see previous comments on Fig. 2.

6.2. Quantification of redundancy of gas sources

Although the cases without external gas disruption have approximately the same probabilistic results for the gas supply, they have different redundancy of the gas sources. The results for the quantification of the redundancy of gas sources are showed in Tables 6 and 7.

Statistical indicators of gas supply are presented in Table 6. The column "L-mean%" of Table 6 represents the relative difference between the physical upper limit of the gas source L and the mean value of the supply. The column is expressed in percentages. The column "cv%" represents the variation coefficient expressed also in

Table 4
Global overview: statistics of overall gas supply. Sorted by vulnerability expressed as D-mean%. The less vulnerable cases are on top.

Case	max	mean	median	std	cv%	D-mean%	D
G	48.5	48.3	48.5	1.6	3.38	0.3	48.5
A	48.5	48.3	48.5	1.6	3.4	0.3	48.5
F	48.5	48.3	48.5	1.6	3.41	0.3	48.5
B	48.5	48.3	48.5	1.7	3.45	0.3	48.5
E	35.5	35.2	35.5	2.6	7.31	15.2	41.5
D	10.5	10.4	10.5	1.2	11.3	75	41.5
C	4	3.95	4	0.44	11.2	90.5	41.5

Table 5
Global overview: Selected probabilities of gas delivery for the case studies. List of demand (D, mcm/d) and probabilities that the gas delivery will be zero or less than 20%, 50%, 80% or 100% of the gas demand. Sorted by vulnerability expressed by the probability of gas delivery. The less vulnerable cases are on the top.

Case	*D*	$P(X=0)$	$P(X<0.2D)$	$P(X<0.5D)$	$P(X<0.8D)$	$P(X<D)$
A	48.46	0	0.000001	0.000002	0.00846	0.0114
G	48.46	0	0	0.000001	0.00839	0.0116
F	48.46	0	0	0.000001	0.00864	0.0117
B	48.46	0.000002	0.000002	0.000003	0.00882	0.0124
E	41.46	0	0.000101	0.00846	0.0217	1
D	41.46	0.0125	0.0134	1	1	1
C	41.46	0.0125	1	1	1	1

Table 6
Statistics of gas sources: reliability quantification of redundancy of gas supply.

Scenario	Source	max	mean	median	std	cv%	L-mean%	Limit L
A	2	30.6	20.3	20.2	0.79	3.88	34.6	31
	10	4	3.95	4	0.44	11.2	1.3	4
	19	25	24.1	24.3	2.2	9.15	3.6	25
B	2	30.6	24.2	24.2	0.68	2.81	21.9	31
	19	25	24.1	24.3	2.2	9.24	3.6	25
C	10	4	3.95	4	0.44	11.2	1.3	4
D	10	10.5	10.4	10.5	1.2	11.3	1.3	10.5
E	10	10.5	10.4	10.5	1.2	11.3	1.3	10.5
	19	25	24.8	25	2.3	9.24	0.8	25
G	2	23.5	15.1	15	0.68	4.48	51.3	31
	10	10.5	2	2.02	0.27	13.4	81	10.5
	11	7.1	7.1	7.1	0	0	0	7.1
	19	25	24.1	24.3	2.2	9.21	3.6	25
F	2	30.6	19.3	19.2	0.86	4.46	37.8	31
	10	10.5	4.94	5	0.57	11.5	53	10.5
	19	25	24.1	24.3	2.2	9.26	3.6	25

percentages. Cases C, D, E have no redundancy of gas sources, so values of "L-mean%" are close to zero. On the contrary, Case G has the largest redundancy, especially thanks to the additional gas source at Node 11, which is used with the largest priority.

Probabilistic indicators of gas supply are presented in Table 7. The table includes the list of gas sources for all cases, their physical upper limit L, and the probabilities that the supply from the source will be zero, represented by the symbol $P(X=0)$, or less than 50%, 80% or 100% of the gas source limit.

Cases C, D, E have no redundancy of gas sources; all the relative probabilities are close to zero. On the contrary, Case G has the largest redundancy, with gas sources at Node 2, at Node 10, and an additional one at Node 11, which is used with the largest priority.

Table 7
Probabilistic analysis of gas sources: Reliability quantification of redundancy of gas supply.

Case	Source	Limit L	$P(X=0)$	$P(X<0.5\ \mathrm{L})$	$P(X<0.8\ \mathrm{L})$	$P(X<L)$
A	2	31	7.30E−05	4.04E−04	9.92E−01	1.00E+00
	10	4	1.23E−02	1.23E−02	1.34E−02	1.39E−02
	19	25	8.29E−03	8.29E−03	8.54E−03	9.99E−01
B	2	31	6.10E−05	3.89E−04	9.91E−01	1.00E+00
	19	25	8.46E−03	8.46E−03	8.68E−03	9.99E−01
C	10	4	1.25E−02	1.25E−02	1.25E−02	1.30E−02
D	10	10.5	1.25E−02	1.25E−02	1.34E−02	1.44E−02
E	10	10.5	1.24E−02	1.24E−02	1.32E−02	1.42E−02
	19	25	8.46E−03	8.46E−03	8.46E−03	8.87E−03
G	2	31	8.60E−05	9.79E−01	1.00E+00	1.00E+00
	10	10.5	1.24E−02	1.00E+00	1.00E+00	1.00E+00
	11	7.1	0.00E+00	0.00E+00	0.00E+00	0.00E+00
	19	25	8.39E−03	8.39E−03	8.65E−03	9.99E−01
F	2	31	6.70E−05	3.94E−04	9.92E−01	1.00E+00
	10	10.5	1.26E−02	9.99E−01	1.00E+00	1.00E+00
	19	25	8.48E−03	8.48E−03	8.75E−03	9.99E−01

6.3. Quantification of probabilistic effects of a new gas infrastructure: a case of LNG terminal

Although cases without external gas disruption have approximately the same CDF of the gas supply at the global (summary) level, they have not only differences on the redundancy of the gas sources, but also significant differences at the node level.

Let us analyse in more detail the probabilistic results of Cases B and F, see Tables 8 and 9. Both cases represent a scenario without external disruption, i.e. input nodes 2 and 19 are supplied as contracted. Moreover, in Scenario F, LNG is added at Node 10 with upper limit 10.5 mcm/d. Node 56 represents a virtual node (summary of supply). As already shown in Table 5, adding the LNG source produces a decrease in $P(X<D)$ from 1.24E−02 to 1.17E−02.

Moreover, results of one million of Monte-Carlo simulations indicate that adding the LNG as redundant supply will diminish the gas delivery uncertainty for Nodes 13, 17, 34, 43 – see Table 9.

However, the quantification of the security of supply effects of the addition of redundant LNG by direct comparison of the probabilities in Tables 8 and 9 is not self-evident, due to size of the tables. For this reason, we created another table, which automatically highlights dissimilarities between see Table 10.

In our approach, the quantification of security of gas supply of the LNG gas infrastructure for node i of the gas network is provided by a risk ratio [27]. The risk ratio is easy to interpret: the risk ratio (also called 'relative risk') for a 'not enough gas event' at Node i is the probability of having 'not enough gas' at Node i without the LNG infrastructure divided by the probability of having 'not enough gas' at Node i with the LNG:

$$risk\_ratio = \frac{P(\text{not enough gas at Node } i \mid \text{no } LNG)}{P(\text{not enough gas at Node } i \mid LNG \text{ is connected})}$$

For example, if the risk ratio equals 5, it is 500% more likely to occur a 'not enough gas event' at Node i when no redundant LNG than in cases with redundant LNG connected, holding all other

Table 8
Results of Scenario B: List of nodes with non-zero demands (D, mcm/d) and probabilities that the node supply will be zero or less than 20%, 50%, 80% or 100% of the node demand.

Node	D	$P(X=0)$	$P(X<0.2D)$	$P(X<0.5D)$	$P(X<0.8D)$	$P(X<D)$
5	3.43	2.00E−06	2.00E−06	1.39E−04	1.39E−04	1.39E−04
6	0.57	3.05E−04	3.05E−04	3.90E−04	3.90E−04	3.90E−04
7	0.66	3.90E−04	3.90E−04	3.90E−04	3.90E−04	3.90E−04
10	2.02	2.27E−04	2.27E−04	2.27E−04	9.35E−04	9.35E−04
13	1.03	2.00E−06	2.00E−06	2.00E−06	2.00E−06	2.00E−06
17	0.46	2.00E−06	2.00E−06	2.00E−06	2.00E−06	2.00E−06
18	8.4	5.00E−06	6.00E−06	7.00E−06	8.46E−03	8.46E−03
21	0.54	8.46E−03	8.46E−03	8.46E−03	8.46E−03	8.46E−03
25	0.6	8.46E−03	8.46E−03	8.46E−03	8.46E−03	8.46E−03
26	0.8	8.58E−03	9.10E−03	9.10E−03	9.10E−03	9.10E−03
27	3.5	8.60E−03	8.60E−03	8.60E−03	8.60E−03	8.60E−03
28	6	8.46E−03	8.46E−03	8.68E−03	8.68E−03	8.68E−03
30	0.4	8.60E−03	8.60E−03	8.60E−03	8.60E−03	8.60E−03
33	0.4	8.60E−03	8.60E−03	8.60E−03	8.93E−03	8.93E−03
34	1	2.00E−06	2.00E−06	2.00E−06	2.00E−06	2.00E−06
36	1.74	2.13E−04	2.13E−04	2.13E−04	2.14E−04	2.15E−04
37	1.3	9.04E−03	9.04E−03	9.04E−03	9.04E−03	9.04E−03
39	1	3.61E−04	3.61E−04	3.61E−04	3.61E−04	3.61E−04
41	0.4	8.99E−03	8.99E−03	8.99E−03	8.99E−03	8.99E−03
42	0.5	9.08E−03	9.08E−03	9.08E−03	9.08E−03	9.08E−03
43	1.06	2.00E−06	2.00E−06	2.00E−06	2.00E−06	2.00E−06
44	2.82	1.39E−04	1.39E−04	2.13E−04	2.76E−04	2.76E−04
47	0.68	1.39E−04	1.39E−04	1.39E−04	1.39E−04	1.39E−04
48	1.17	7.00E−06	7.00E−06	7.00E−06	7.00E−06	7.00E−06
51	7	3.90E−04	3.90E−04	3.90E−04	6.18E−04	6.18E−04
52	0.98	3.20E−05	3.20E−05	3.20E−05	3.40E−05	3.40E−05
56	48.46	2.00E−06	2.00E−06	3.00E−06	8.82E−03	1.24E−02

Table 9
Results of Scenario F: List of nodes with non-zero demands (D, mcm/d) and probabilities that the node supply will be zero or less than 20%, 50%, 80% or 100% of the node demand.

Node	D	$P(X=0)$	$P(X<0.2D)$	$P(X<0.5D)$	$P(X<0.8D)$	$P(X<D)$
5	3.43	0.00E+00	0.00E+00	3.00E−06	3.00E−06	3.00E−06
6	0.57	3.00E−06	3.00E−06	4.00E−06	4.00E−06	4.00E−06
7	0.66	7.40E−05	7.40E−05	7.40E−05	7.40E−05	7.40E−05
10	2.02	4.00E−06	4.00E−06	4.00E−06	4.00E−06	4.00E−06
13	1.03	0.00E+00	0.00E+00	0.00E+00	0.00E+00	0.00E+00
17	0.46	0.00E+00	0.00E+00	0.00E+00	0.00E+00	0.00E+00
18	8.4	0.00E+00	0.00E+00	0.00E+00	8.48E−03	8.48E−03
21	0.54	8.48E−03	8.48E−03	8.48E−03	8.48E−03	8.48E−03
25	0.6	8.49E−03	8.49E−03	8.49E−03	8.49E−03	8.49E−03
26	0.8	8.64E−03	9.14E−03	9.14E−03	9.14E−03	9.14E−03
27	3.5	8.64E−03	8.64E−03	8.64E−03	8.64E−03	8.64E−03
28	6	8.49E−03	8.49E−03	8.75E−03	8.75E−03	8.75E−03
30	0.4	8.64E−03	8.64E−03	8.64E−03	8.64E−03	8.64E−03
33	0.4	8.64E−03	8.64E−03	8.64E−03	8.99E−03	8.99E−03
34	1	0.00E+00	0.00E+00	0.00E+00	0.00E+00	0.00E+00
36	1.74	3.00E−06	3.00E−06	7.30E−05	2.26E−04	2.27E−04
37	1.3	9.10E−03	9.10E−03	9.10E−03	9.10E−03	9.10E−03
39	1	3.47E−04	3.47E−04	3.47E−04	3.47E−04	3.47E−04
41	0.4	8.98E−03	8.98E−03	8.98E−03	8.98E−03	8.98E−03
42	0.5	9.04E−03	9.04E−03	9.04E−03	9.04E−03	9.04E−03
43	1.06	0.00E+00	0.00E+00	0.00E+00	0.00E+00	0.00E+00
44	2.82	3.00E−06	3.00E−06	3.00E−06	3.00E−06	3.00E−06
47	0.68	3.00E−06	3.00E−06	3.00E−06	3.00E−06	3.00E−06
48	1.17	6.00E−06	6.00E−06	6.00E−06	6.00E−06	6.00E−06
51	7	2.28E−04	2.86E−04	3.21E−04	3.99E−04	3.99E−04
52	0.98	3.50E−05	3.50E−05	3.50E−05	3.50E−05	3.50E−05
56	48.46	0.00E+00	0.00E+00	1.00E−06	8.64E−03	1.17E−02

Table 10
Quantifications of probabilistic effects of an 10.5 mln/d LNG source. Positively affected demand nodes highlighted.

Node	**D**	$rr(X=0)$	$rr(X<0.2D)$	$rr(X<0.5D)$	$rr(X<0.8D)$	$rr(X<D)$
5	3.43	–	–	46.3	46.3	46.3
6	0.57	101.7	101.7	97.5	97.5	97.5
7	0.66	5.3	5.3	5.3	5.3	5.3
10	2.02	56.8	56.8	56.8	233.8	233.8
13	1.03	–	–	–	–	–
17	0.46	–	–	–	–	–
18	8.4	–	–	–	1.0	1.0
21	0.54	1.0	1.0	1.0	1.0	1.0
25	0.6	1.0	1.0	1.0	1.0	1.0
26	0.8	1.0	1.0	1.0	1.0	1.0
27	3.5	1.0	1.0	1.0	1.0	1.0
28	6	1.0	1.0	1.0	1.0	1.0
30	0.4	1.0	1.0	1.0	1.0	1.0
33	0.4	1.0	1.0	1.0	1.0	1.0
34	1	–	–	–	–	–
36	1.74	71.0	71.0	2.9	0.9	0.9
37	1.3	1.0	1.0	1.0	1.0	1.0
39	1	1.0	1.0	1.0	1.0	1.0
41	0.4	1.0	1.0	1.0	1.0	1.0
42	0.5	1.0	1.0	1.0	1.0	1.0
43	1.06	–	–	–	–	–
44	2.82	46.3	46.3	71.0	92.0	92.0
47	0.68	46.3	46.3	46.3	46.3	46.3
48	1.17	1.2	1.2	1.2	1.2	1.2
51	7	1.7	1.4	1.2	1.5	1.5
52	0.98	0.9	0.9	0.9	1.0	1.0
56	48.46	–	–	3.0	1.0	1.1

variables constant. On the contrary, a relative risk of one at Node *i* means that the LNG infrastructure has no effect on the Node *i*.

As shown in Table 10, if we compare simulations with and without LNG, the risk ratio (expressed by the symbol "*rr*") of having less than 80 % of the demand at Node 6 is, approximately, 97. Naturally, the largest effect of having the LNG infrastructure is directly visible at Node 10. Moreover, the positive effect of LNG is evident also for Nodes 5-7, 44, 47 and, partially, also for Node 36. The results appear to be realistic: As expected, the nodes showing positively effects are those geographically close to the LNG.

Finally, the nodes with relative risk equal to one are not affected by the LNG. For Node 52, and, partially, for Node 36, the relative risk is close to 0.9, considering the inherent numerical approximation of the Monte-Carlo method. But it is not a supply gas problem, as the estimated non-delivery probabilities at these two nodes are very close to zero.

7. Conclusions and future work

The paper describes the methodological approach and the results obtained by the probabilistic gas network simulator ProGasNet. The presented Monte-Carlo simulation technique for stochastic network model with a priority supply pattern represents a general approach, which can be used with advanced failure models. The here presented failure model currently does not depend on the component state (age, overload). Currently we do not simulate repair of the failed components. Currently one damage level (complete damage) is considered for pipelines. In the future, a multi-state approach will be analysed. Even with these simplifications, the model is able to identify critical network nodes in terms of security of supply.

Our repeated numerical experiments indicate that 1 million of runs are enough for the presented gas network: For example, it is possible to provide a detailed quantification of probabilistic effects of a new gas infrastructure. Generally, quality of results of the Monte-Carlo simulations can be analysed by exact confidence limits [31].

The ProGasNet model provides a quantitative indication of the worst networks nodes in terms of security of gas supply and provides their numerical ranking. The same model can be applied for many other purposes, like vulnerability analysis, bottleneck analysis, evaluation of new network development plans and the analysis of potential supply crisis.

The ProGasNet has been applied to a test case based on the real gas transmission network of some EU countries. The results obtained indicate the benefits that might derive from the insertion of a new infrastructure (LNG terminal) to an existing network and in particular to certain nodes. It is important to note that security of supply also depends on redundancy of supply sources, and that this can be quantified by the model proposed.

The model will be expanded and improved in many directions in the future, in particular by integrating more results from physical flow models (important for larger networks containing many compressor stations) and optimising the algorithm to handle more MC runs.

Acknowledgement

We thank the anonymous reviewers for their careful reading of our manuscript and their many insightful comments and suggestions.

References

[1] Regulation (EU) No. 994/2010 of the European Parliament and of the Council of 20 October 2010 concerning measures to safeguard security of gas supply and repealing Council Directive 2004/67/EC. Official Journal of the European Union; 2010.
[2] Lewis AM, Ward D, Cyra L, Kourti N. European reference network for critical infrastructure protection. Int J Crit Infrastruct Prot 2013;6:51–60.
[3] Setola R, De Porcellinis S, Sforna M. Critical infrastructure dependency assessment using the input–output inoperability model. Int J Crit Infrastruct Prot 2009;2:170–8.
[4] Ouyang M. Review on modeling and simulation of interdependent critical infrastructure systems. Reliab Eng Syst Saf 2014;121:43–60.
[5] Trucco P, Cagno E, De Ambroggi M. Dynamic functional modelling of vulnerability and interoperability of Critical Infrastructures. Reliab Eng Syst Saf 2012;105:51–63.
[6] Cakir Erdener B, Pambour KA, Bolado Lavin R, Dengiz B. Electr Power Energy Syst 2014;61:410–20.
[7] Ball MO, Colbourn CJ, Provan JS. Network reliability. College Park, MD, USA: University of Maryland; 1992.
[8] Aven T. Availability evaluation of oil/gas production and transportation systems. Reliab Eng Syst Saf 1987;18:35–44.
[9] Johansson J, Hassel H, Zio E. Reliability and vulnerability analyses of critical infrastructures: comparing two approaches in the context of power systems. Reliab Eng Syst Saf 2013;120:27–38.
[10] Wei-Chang Y, Changseok B, Chia-Ling H. A new cut-based algorithm for the multi-state flow network. Reliab Eng Syst Saf 2015;136:1–7.
[11] Woldeyohannes AD, Majid MAA. Simulation model for natural gas transmission pipeline network system. Simul Model Pract Theory1569-190X 2011;19(1):196–212. http://dx.doi.org/10.1016/j.simpat.2010.06.006.
[12] Luis F, Ayala H, Leong Chew Y. A robust linear-pressure analogue for the analysis of natural gas transportation networks. J Nat Gas Sci Eng1875-5100 2013;14:174–84. http://dx.doi.org/10.1016/j.jngse.2013.06.008.
[13] Kabirian A, Hemmati MR. A strategic planning model for natural gas transmission networks. Energy Policy0301-4215 2007;35(11):5656–70. http://dx.doi.org/10.1016/j.enpol.2007.05.022.
[14] Ouyang M, Dueñas-Osorio L. An approach to design interface topologies across interdependent urban infrastructure systems. Reliab Eng Syst Saf 2011;96(11):1462–73. http://dx.doi.org/10.1016/j.ress.2011.06.002.
[15] Todinov MT. Flow networks: analysis and optimisation of repairable flow networks, networks with disturbed flows, static flow networks and reliability networks. London, UK: Elsevier; 978-0-12-398396-1.
[16] Kopustinskas V, Praks P. Development of gas network reliability model. JRC technical report JRC78151Luxembourg: European Commission; 2012.
[17] Praks P, Kopustinskas V. Development of a gas transmission network reliability model: a case study. In: Proceedings of the ESREL'2013 conference – Steenbergen et al. (Eds.). Taylor & Francis Group, London; 978-1-138-00123-7; 2014. p. 2177–2183.

[18] Ahuja RK, Magnanti TL, Orlin JB. Network flows. In: Nemhauser GL, Rinnooy Kan MJ, Todd MJ, editors. New York: Elsevier North-Holland Inc.; 1989. p. 211–369.
[19] Bazaraa MS, Jarvis JJ, Sherali HD. Linear programming and network flows. New York: John Wiley & Sons; 2010.
[20] Deo N. Graph theory with applications to engineering with computer science. Upper Saddle River, NJ, USA: Prentice Hall; 2008.
[21] Golub GH, Van Loan CF. Matrix computations. Baltimore: Johns Hopkins University Press; 1996.
[22] EGIG report, 8th Report of the european gas pipeline incident data group; Groningen; 2011.
[23] Pelletier C, Wortmann JC. A risk analysis for gas transport network planning expansion under regulatory uncertainty in Western Europe. Energy Policy 2009;37(2):721–32.
[24] MJ Jung, JH Cho, W Ryu LNG terminal design feedback from operator's practical improvements. In: Proceedings of the 22nd world gas congress; Tokyo, Japan; 2003.
[25] Definition of available capacities at interconnection points in liberalized market. Gas transmission europe; July 2, 2004; Ref.: 04CA041-final.
[26] Rubinov M, Sporns O. Complex network measures of brain connectivity: uses and interpretations. NeuroImage 2010;52:1059–69.
[27] Norton EC, Wang H, Ai C. Computing interaction effects and standard errors in logit and probit models. Stata J 2004;4(2):154–67.
[28] Praks P, Kopustinskas, V. Monte-Carlo based reliability modelling of a gas network using graph theory approach. In: Proceedings of the 9th international conference on availability, reliability and security; University of Fribourg, Switzerland; 10.1109/ARES.2014.57; 978-1-4799-4223-7; Sept. 8–12, 2014. p. 380–386
[29] Kopustinskas V, Praks, P. Time dependent gas transmission network probabilistic simulator: focus on storage discharge modeling. In: Proceedings of the european safety and reliability conference ESREL 2014; Wroclaw, Poland (Safety and Reliability: Methodology and Applications – Nowakowski et al. (Eds) © 2015 Taylor & Francis Group, London; 978-1-138-02681-0; 14–18th Sept. 2014. p. 2069–2075.
[30] Praks P, Contini S, Kopustinskas V. Monte Carlo and fault tree aproaches in reliability applications of gas transmission network. In: Proceedings of the 2014 15th international scientific conference on electric power engineering, EPE art. no. 6839421; 10.1109/EPE.2014.6839421; 2014. p. 69–74.
[31] Dubčáková R, Praks P, Moučka L. Statistical model of quality of radon measurements using electret ion chamber detectors. art. no. ncr058. Radiat Prot Dosim 2011;145(2–3):295–9. http://dx.doi.org/10.1093/rpd/ncr058.